Biochemical and Biophysical Research Communications 459 (2015) 424–429

Contents lists available at ScienceDirect

Biochemical and Biophysical Research Communications

journal homepage: www.elsevier.com/locate/ybbrc

Cross talk between *Leishmania donovani* CpG DNA and Toll-like receptor 9: An immunoinformatics approach

Chhedi Lal Gupta [a], Salman Akhtar [b], Andrew Waye [c, e], Nihar R. Pandey [d, e], Neelam Pathak [a], Preeti Bajpai [a, *]

[a] Department of Biosciences, Integral University, Lucknow, 226026, UP, India
[b] Department of Bioengineering, Integral University, Lucknow, 226026, UP, India
[c] Department of Biology, University of Ottawa, 30 Marie-Curie, Ottawa, ON, K1N 6N5, Canada
[d] Center for Stroke Recovery, Ottawa Hospital Research Institute and Department of Medicine, University of Ottawa, Ottawa, Ontario, Canada
[e] Medipure Pharmaceuticals Inc., Maple Ridge, BC, V2X 2Z3, Canada

ARTICLE INFO

Article history:
Received 7 February 2015
Available online 28 February 2015

Keywords:
Toll-like receptor
Immune response
PAMPs
Homology modeling
Parasitic infection

ABSTRACT

The precise and potential contribution of Toll-like receptors (TLRs) signaling pathways in fighting parasitic infections of *Leishmania spp.*, an intracellular protozoan parasite, has gained significant attention during the last decades. Although it is well established that TLR9 recognizes CpG motifs in microbial genomes, the specificity of the CpG DNA pattern of *Leishmania* parasite interacting with endosomal TLR9 is still unknown. Hence in our study to identify the CpG DNA pattern of *Leishmania donovani* acting as ligand for TLR9, consecutive homology searches were performed using known CpG ODN 2216 as initial template until a consistent CpG pattern in *L. donovani* was found. A reliable model of TLR9 ectodomains (ECDs) as well as CpG DNA patterns was predicted to develop the 3D structural complexes of TLR9 ECD–CpG DNA utilizing molecular modeling and docking approaches. The results revealed the preferential specificity of *L. donovani* CpG DNA to TLR9 compared to control ODN and other CpG patterns. The interface between TLR9 and *L. donovani* CpG DNA was also found to be geometrically complementary with the LRR11 region of TLR9, acting as the critical region for ligand recognition. The *L. donovani* CpG pattern identified can be employed to derive a platform for development of an innate immunomodulatory agent for deadly disease.

1. Introduction

The recognition of pathogen associated molecular patterns (PAMPs) by Toll-like receptors initiate intracellular signal transduction pathways to trigger expression of genes to direct innate immune responses [1]. To date, thirteen TLR members (TLR1-13) have been identified on the surface (TLR 1, 2, 4, 5, and 6) or within the endosomal compartment (TLR 3, 7, 8, and 9) of TLR-expressing cells. Cell surface TLRs recognize structural components of pathogens, while endosomal TLRs are specific to pathogenic nucleic acid recognition [2]. TLRs are type I transmembrane glycoproteins consisting of an extracellular domain/ectodomain (ECD) which is the binding site for ligands of various microbial pathogens, a single transmembrane spanning segment, and a globular cytoplasmic Toll/interleukin (IL)-1 receptor (TIR) domain [3]. The ECD of TLR is composed of 19–27 leucine-rich repeats (LRR) motifs forming a loop with conserved hydrophobic residues pointing inward. Several loops form a horseshoe-shaped ECD, which is N- and C-terminally flanked by cysteine flanking regions [4].

An endosomally expressed TLR9, one of the thirteen mammalian TLRs serves as a receptor for microbial CpG-DNA/CpG-containing oligodeoxynucleotides (CpG-ODN) [5]. Recognized CpG-DNA within the endosome initiates signaling via the sequential recruitment of MyD88 and TRAF6, thereby activating downstream nuclear transcription factors NF-kB and AP-1 which instigates inflammatory cytokine (TNF-α, IL-6, IL-1β, and IL-12) induction [6,7]. Synthetic CpG-ODN mimics the stimulatory effect of microbial DNA, inducing both lymphoid and myeloid lineage proliferation [8]. The ECD of TLR9 comprises 25 LRRs contributing to the binding of ligand. However, it is still unknown which LRR and their specific amino acids are involved in interaction with the pathogenic fragment [9].

* Corresponding author.
E-mail addresses: preeti2874@gmail.com, pbajpai@iul.ac.in (P. Bajpai).

http://dx.doi.org/10.1016/j.bbrc.2015.02.121
0006-291X/

Parasitic protozoans of *Leishmania* species affect around 350 million people in 98 countries and have been a matter of serious concern [10]. This intracellular parasite is capable of presenting a broad range of clinical manifestations from cutaneous lesions to fatal visceral disease, with the immune status of the host largely determining severity [11]. Existing therapeutic strategies are limited due to higher treatment cost, restricted use, as well as drug resistance [12]. The innate immune response has been the preferred target for vaccine/drug development against *Leishmania* [13].

TLRs are considered to be the first step of the innate immune response against *Leishmania* by hampering the parasite's ability to trigger a Th1 immune response [14]. The parasitic components LPG, GPIL, and gp63 are thought to be the first substrates to encounter the innate immune system via TLR2/4 [15] and the activation of myeloid and plasmacytoid DCs in a strictly TLR9-dependent manner against *Leishmania spp.* has also been observed [16,17]. Another study demonstrated the increased expression of TLR9 after exposure of macrophages to *Leishmania* DNA thereby establishing the role of TLR9 as a mechanism for host innate immune response against the parasite [18]. However, the specificity of the parasitic DNA pattern to TLR9 is still unexplored. The present study was therefore focused on the prediction of a common structural pattern (CpG DNA) for TLR9 recognition in *L. spp.* by applying CpG ODN-2216 as initial template using a homology searching method. Further molecular modeling and docking studies were employed to model the TLR9 ECD–CpG DNA complexes to elucidate the critical residues of TLR9 ECD implicated for molecular interaction.

2. Materials and methods

2.1. Homology search and ssDNA modeling

The CpG ODN 2216 a class A human specific agonist (ligand) of TLR9 was selected as a initial template for homologous search of parasitic DNA pattern using BLAST online server (http://blast.ncbi.nlm.nih.gov/Blast.cgi). The functional protocol is diagrammatically represented in Fig. 1. The Macromolecules tool in Discovery Studio Visualizer 3.1 was employed to build the model of CpG ODN 2216 and screened parasitic sequences. Previous reports indicate that the immunostimulatory activity of TLR9 depends on the single stranded character of CpG DNA [19]. Hence we modeled the template and identified DNA sequences as a single stranded molecule using standard helix parameters in the B-form.

2.2. Structural modeling and validation of TLR9 ectodomains

The 3D structural details of human and mouse TLR9 are still unexplored, thereby it was essential to develop the 3D structures of these TLRs to explore their molecular functions. The protein sequences of human and mouse TLR9 (hTLR9 and mTLR9) were retrieved from UniProt database, having accession numbers of Q9NR96 and Q9EQU3 respectively. The 3D structure of the ectodomains of hTLR9 and mTLR9 were developed by I-TASSER online server. I-TASSER was ranked as No. 1 server for protein structure prediction as it incorporates threading, *ab initio* modeling, comparative modeling, and structural refinement [20].

The backbone conformation of the modeled structures were calculated by analyzing the phi (Φ) and psi (ψ) torsion angles using Procheck program, as determined by Ramachandran plot statistics [21]. The ProSA web server (https://prosa.services.came.sbg.ac.at/prosa.php) was employed to verify the structure in terms of Z score, representing the overall quality and deviation of total energy. The reliability of the modeled structures were also assessed by ProQ (http://www.sbc.su.se/~bjornw/ProQ/ProQ.html) server, which is a neural network-based predictor based on a number of structural features to predict the quality of a protein model in term of LG and MaxSub Scores.

2.3. Construction and analysis of Protein-DNA complexes

The complexes were developed by using the HEX docking server based on a rigid body docking algorithm that determines the steric shape, electrostatic potential, and charge density of the protein as expansions of spherical polar Fast Fourier Transformation (FFT) basis functions [22]. In Hex's docking calculations, the TLR9 ECD was defined as receptor and DNA patterns as the ligands. The docking parameters used for this investigation were shape plus electrostatics correlation type with 25 search orders, receptor range angle 180, ligand range angle 180, and step size 7.5. Other parameters were set as the default mode. The molecular interactions of TLR9 ECD–CpG DNA docked complexes were analyzed by

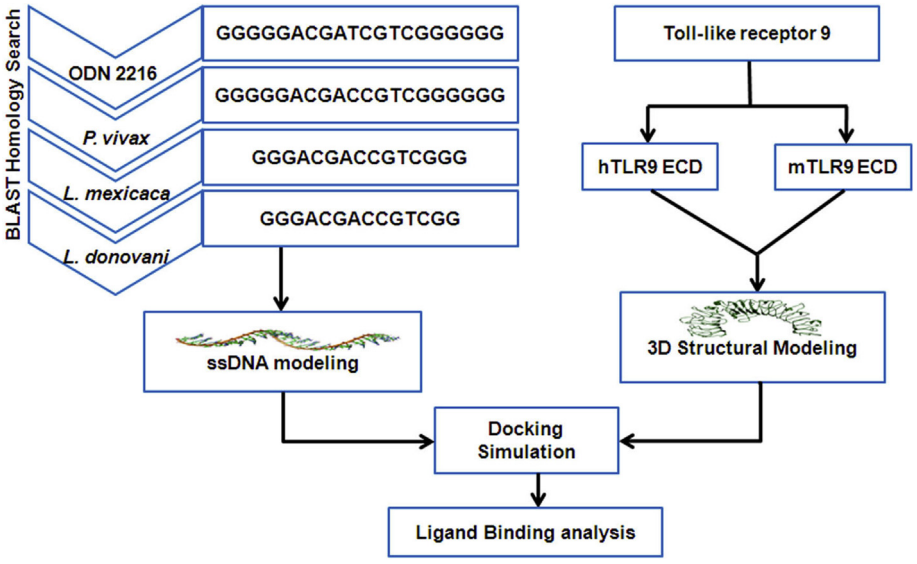

Fig. 1. Pictorial representation of the methodology employed for the study.

calculating the hydrophobic contacts and intermolecular hydrogen bond interactions. The LigPlot + version v.1.4.4 tool was employed to calculate the hydrophobic contacts [23]. The intermolecular hydrogen bond calculations and protein structure illustrations were performed using Discovery Studio Visualizer 3.1. The PatchDock molecular docking algorithm based on shape complementarity principles was used as an alternative docking method to corroborate the results. The binding energy was calculated as Atomic contact energy (ACE) [24].

3. Results

3.1. Identification of Leishmania donovani CpG DNA pattern

It is well established that the innate immune mediator TLR9 expressed in the endosomal compartment recognizes DNA fragments (CpG motifs) of parasitic origin. For the identification of *L. donovani* CpG DNA pattern recognized by TLR9, the BLAST search was performed using CpG ODN 2216 as template and screened a homologous pattern present in the chromosome 1 (550363–550382 position) of *Plasmodium vivax* (*P. vivax*) SaI-1 strain genome. This homologous pattern of *P. vivax* was used as template for BLAST search of an identical pattern (15 bp) from *Leishmania mexicana* (*L. mexicana*) MHOM/GT/2001/U1103 complete genome, chromosome 12 (208412–208398 position). This pattern of *L. mexicana* was then screened and to get the homologous sequence (14 bp) in *L. donovani* (*L. donovani*) BPK282A1 complete genome, chromosome 12 (215284–215271 position) (Fig. 1). The sequence alignment of these parasitic sequences with CpG ODN 2216, as depicted in Fig. 2, revealed the conserved nucleotides with a single base pair variation. Furthermore, the similarity matrix between these sequences was also prepared and presented in Supplementary Table 1 in which the CpG pattern of *L. donovani* represents 92.86% similarity with known ligand (CpG ODN 2216).

3.2. Structural analysis of ectodomains

The full length TLR9 protein is composed of 1032 amino acids including a signal peptide of 25 amino acids (1–25 aa). The mature TLR9 protein ECD, trans-membrane (TM) and TIR domain are 26–818, 819–839 and 868–1016 amino acids respectively. The automated 3D structure of ECDs from hTLR9 and mTLR9 were predicted by I-TASSER server which employs a fragment-based method for modeling of protein structures. A hierarchical approach was used to excise the fragments from multiple template structures and threading alignments [25]. The structural modeling of hTLR9 ECD were carried out using TLR8 crystal structure (PDB_ID 3W3G) and TLR5 crystal structure (PDB_ID 3J0A), while mTLR9 ECD modeling was performed with TLR8 crystal structure (PDB_ID 3W3G and 3W3J) and TLR3 crystal structure (PDB_ID 2A0Z). The

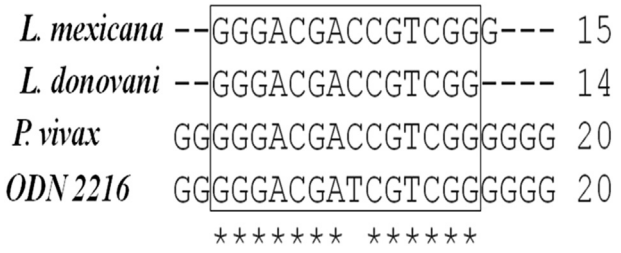

Fig. 2. Multiple sequence alignment of CpG ODN 2216 and DNA patterns of *P. vivax, L. mexicana* and *L. donovani* using Clustal W tool. The asterisk represents conserved sequences.

server predicted five models of TLR9 ECDs with their C-score in which the models having higher C-score values were selected. High C-score value is directly proportional to the confidence level of model [20]. The structural alignment of these templates with TLR9 ECDs as identified by TM-align tool (http://zhanglab.ccmb.med.umich.edu/TM-align/) indicated that predicted ECD of hTLR9 had a TM score (0.719) & root mean square distance (RMSD) (0.73 Å) with TLR8 crystal structure, and a TM score (0.456) & RMSD (5.36 Å) with TLR5 crystal structure, and ECD of mTLR9 had a TM score (0.935) & RMSD (0.74 Å) with TLR8 crystal structure, and a TM score (0.622) & RMSD (4.98 Å) with TLR3 crystal structure. This small number of TM score and RMSD represents that the developed models have a similar structural pattern with templates.

We also validated the developed models with Procheck, ProQ and ProSA servers for reliability (Supplementary Table 2). The steriochemical validation of the developed models using Procheck program (which generates a Ramachandran plot), indicated that 75.0% and 76.3% amino acid residues of hTLR9 and mTLR9 models respectively were in the most favored regions of the plot whereas 0.0% of the residues were in disallowed regions. The Z score obtained by ProSA server represents the overall quality and measures the deviation of the total energy of protein structure. The Z score values of the predicted models were −3.51 and −6.76 for hTLR9 and mTLR9 respectively, which lies in the acceptable range of −10 to 10. The predicted LG score (4.330 for hTLR9 & 5.498 for mTLR9) obtained by ProQ server was also found to be extremely good. These results clearly propose that the obtained models are consistent and can be considered for further studies.

3.3. Identification of TLR9 ligand recognition sites

Characterizing complex molecular binding processes are important to understanding protein-ligand interactions and concerted efforts have been made using both experimental and computational approaches [26]. The output of Hex server consists of clusters of TLR9-CpG DNA complexes which were analyzed by ligand position, orientation and closer amino acids interactions. The cluster with the best solution of interaction was selected. Similarly the PatchDock produced geometric score, interface area size and ACE of the solutions using clustering by transformation parameters and RMSD method. However, the cluster population is generally not defined by the server. Subsequently the docked complexes of human and mouse TLR9 ECD–CpG DNA were characterized in terms of the interaction features to elucidate the mechanism of TLR9–CpG DNA recognition. The hydrophobic and hydrogen bond interaction analysis demonstrated that the TLR9 ECD–CpG DNA interaction sites were located near the central region of the TLR9 ECD (Fig. 3A and B). The residues involved in hydrophobic interactions between both human and mouse TLR9 ECD–CpG DNA complexes are demonstrated in Table 1. This interaction revealed that both docked energy (−553.33 and −552.94 Kj/mol) and ACE (−223.51 and −296.92 kcal/mol) exhibited by the *L. donovani* CpG DNA pattern with hTLR9 and mTLR9 complex was minimal as compared to the other complexes considered, signifying robust protein-ligand binding (Table 1). To ascertain that the single base pair change in the *L. donovani* CpG pattern is not responsible for its better binding affinity, 14 parallel docking calculations using both the servers were performed with 14 different DNA fragments. Each fragment was constructed by randomly replacing one base-pair at a time (G⇌A & C⇌T). Among these altered fragments three were found to be present in chromosome 16, 21 and 26 respectively whereas the rest were hypothetical (Supplementary Table 3). These docking models also demonstrated that the minimum docked energy and ACE is exhibited by the conserved *L. donovani* CpG pattern.

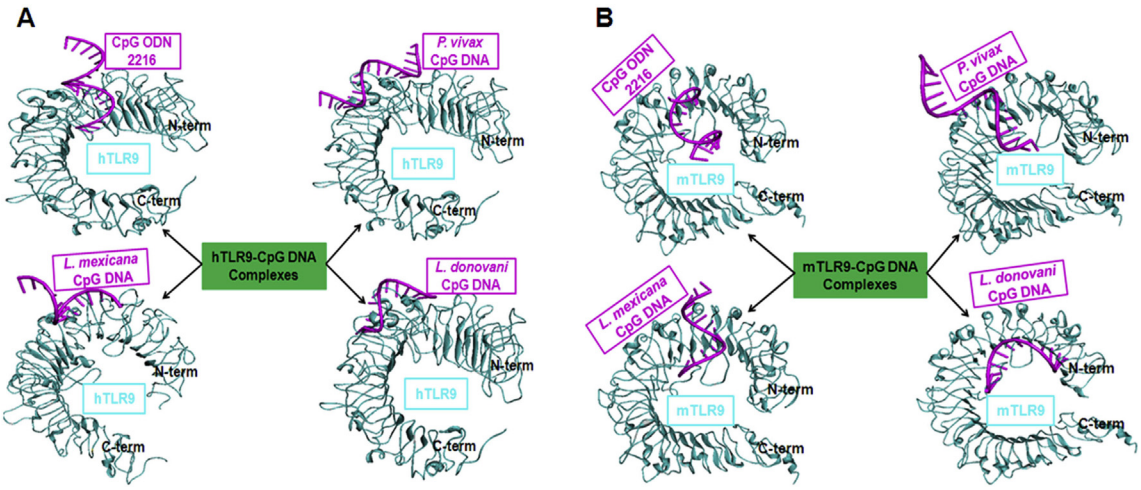

Fig. 3. Structural complexes of TLR9 ECDs (in cyan color) with CpG DNA patterns (in magenta color) developed by molecular modeling and docking approach. **(A)** Complexes of hTLR9 with CpG DNA and **(B)** mTLR9 with CpG DNA. (For interpretation of the references to color in this figure legend, the reader is referred to the web version of this article.)

Table 1
Molecular docking studies of CpG DNA patterns with TLR9.

Complexes	Hex Docking server				PatchDock server			Residues making hydrophobic contact
	No. of generated solutions	No. of clusters[#]	Cluster no. with best solution	Docking energy (Kj/mol)	Score	Area (Å^2)	ACE* (Kcal/mol)	
hTLR9–CpG ODN 2216	3000	15	4	−423.76	8392	954.00	−149.55	Glu223, Cys268, Asn300, Ser302, Gly308, Leu310, Lys328
hTLR9–*P. vivax* CpG DNA	3000	15	4	−420.98	8400	1102.70	−125.76	Leu226, His276, Asn300, Ala301, Trp303, Ile324, Thr327, Leu379, Ala388
hTLR9–*L. mexicana* CpG DNA	3000	15	11	−368.01	8510	1112.10	−202.25	Glu223, Cys268, Pro269, Ile324, Thr327, Phe376, Leu379
hTLR9–*L. donovani* CpG DNA	3000	15	1	−553.33	8800	1132.40	−223.51	Gln274, Asn300, Ala301, Cys323, Thr327, Lys328, Leu384, Ala388, Arg389, Leu408, Ala413
mTLR9–CpG ODN 2216	1800	9	2	−397.92	9326	1130.70	−171.64	Trp96, Phe173, Lys207, Glu287, Arg337, Ala457, Leu459
mTLR9–*P. vivax* CpG DNA	1800	9	5	−320.70	9128	1113.20	−121.41	Thr325, His326, Phe343, Lys347, Tyr382
mTLR9–*L.mexicana* CpG DNA	2000	10	3	−373.76	9628	1217.80	−290.42	Glu223, Tyr224, Val248, Val308, Arg335, Lys338, Pro454, His455, Pro456, Ser460, Pro462, Asp469, Lys472
mTLR9–*L. donovani* CpG DNA	2000	10	2	−552.94	9634	1218.10	−296.92	Gly176, Tyr180, Lys181, Tyr208, Cys258, Asp259, Ile266, Arg346, Phe375

Note: [#]Each cluster contains 200 solutions, *ACE–Atomic contact energy.

The presence of hydrogen bonds (HB) frequently contributes to the stability of protein-ligand complexes. The HB interactions between hTLR9 ECD–CpG DNA complexes by Hex server presented in Supplementary Tables 4 and 5 revealed that hTLR9 ASN309, GLN335, ARG348 donor atoms formed HB with DG2, DG3, DG4, DT13 acceptor atoms of CpG ODN 2216; GLN274, ARG348, ARG385 donor atoms of hTLR9 formed HB with DA6, DC14, DG15, DG16 acceptor atoms of *P. vivax* CpG DNA; hTLR9 CYS323, ARG348 donor atoms formed HB with DC5, DG6 acceptor atoms of *L. mexicana* CpG DNA and its acceptor atoms TYR321, CYS323 formed HB with DG6 donor atoms of *L. mexicana* CpG DNA; and ARG348, HIS372, ARG385 donor atoms of hTLR9 formed HB with DG2, DA4, DC12, DG13 acceptor atoms of *L. donovani* CpG DNA. The interactions between mTLR9 ECD-CpG DNA complexes proposed that mTLR9 ARG247, ARG337 donor atoms produced HB with DG12, DC14 acceptor atoms of CpG ODN 2216; ARG257, LYS348, HIS355 donor atoms of mTLR9 created HB with DG1, DG4, DC11 acceptor atoms of *P. vivax* CpG DNA; mTLR9 ARG335 donor atoms formed HB with DA acceptor atoms of *L. mexicana* CpG DNA and its acceptor atom ASP469 formed HB with donor atom DG15 of *L. mexicana* CpG DNA; and ARG257, TYR345, LYS347 donor atoms of mTLR9 formed HB with DC8, DC9, DG10, DT11 acceptor atoms of *L. donovani* CpG DNA and its acceptor atoms GLU267 formed HB with DG6 donor atom of *L. donovani* CpG DNA.

3.4. LRR11 region critical for ligand recognition

The particular LRR regions of TLR9 responsible for molecular interactions with CpG DNA's were scrutinized to explore the most preferred site by all the DNA patterns. The results demonstrated that in hTLR9 specific amino acid residues within, LRR10 & -11 are responsible for binding with CpG ODN 2216; LRR8, -11 & -12 with *P. vivax* CpG DNA; LRR10 & -11 with *L. mexicana* CpG DNA; and LRR11 & -12 with *L. donovani* CpG DNA (Fig. 4A). When mTLR9 was examined, LRR8 & -11 were determined to be responsible for recognition of CpG ODN 2216 and *P. vivax* CpG DNA; LRR11 & -15 for

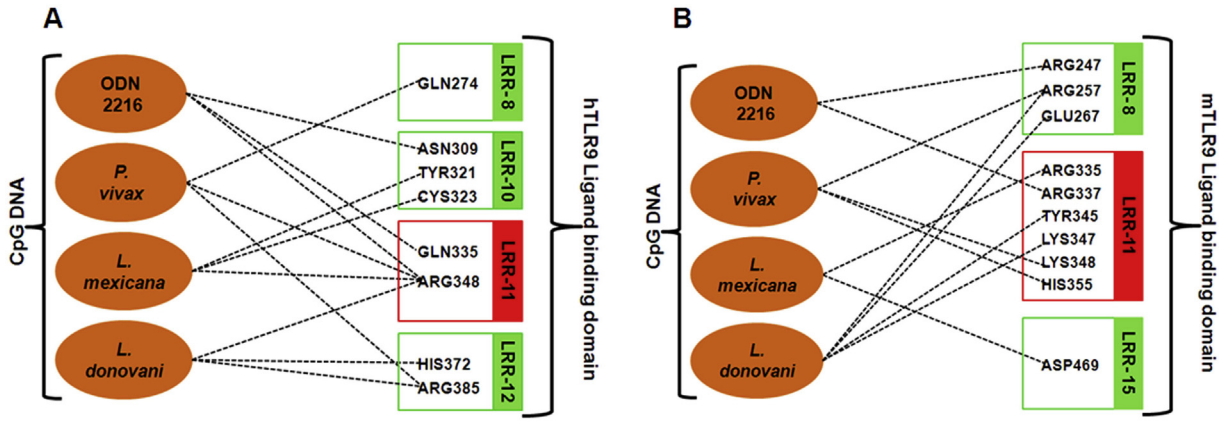

Fig. 4. Diagrammatic representation of amino acid residues in LRR regions of TLR9 ECD in interaction with ligands (CPG DNA) **(A)** hTLR9 LRR region and (**B**) mTLR9 LRR region. The black dash lines indicate hydrogen bond interactions between TLR9 LRR region and ligands. The LRR11 region of TLR9 (highlighted in red color) has been found to be critically involved in all the interactions. (For interpretation of the references to color in this figure legend, the reader is referred to the web version of this article.)

L. mexicana CpG DNA; and LRR8 & -11 for *L. donovani* CpG DNA (Fig. 4B). The alternative docking tool also demonstrated almost similar residues of LRR11 region of TLR9 forming HB interactions with ligands indicating towards comparable pattern of interactions in both these docking strategies (Supplementary Tables 4 and 5). Previous reports indicated that TLR9 activation is mediated by LRR2, -5, -8 and -13–CpG DNA interaction [27,28]. However, a recent report by Pan et al. (2012) verified that only LRR11 of TLR9 had the highest affinity for CpG ODN. Our results therefore coincide with this report certifying the contribution of LRR11 region of hTLR9 and mTLR9 for the recognition of each ligands considered for this study rather than LRR8, -10, -12 and -15, indicating it as critical region.

4. Discussion

The available literature to date indicates an important role of TLR9 in detecting *Leishmania* DNA to initiate the innate immune response [18,29,30]. Recent reports have documented that the recognition of *L. spp.* molecules by TLR9 triggers the early NK cell response to infection dependent upon the expression of IL-12 by myeloid DCs [16,17]. Studies on *Leishmania* antiparasitic strategies also pointed towards the inclusion of synthetic oligonucleotides along with potential therapeutic and vaccine agents since synthetic CpG-ODN mimics the stimulatory activity of CpG-DNA [31,32]. In addition, enhanced rIL18 expression dependent on the synergistic role of CpG motifs has also been observed [13]. The specific CpG DNA sequence pattern recognized by TLR9 from *L. spp.* is still matter of debate. Therefore, this study was focused for the identification of CpG DNA patterns in *L. donovani* that may act as ligands for TLR9. We performed a homology searching method with BLAST employing known TLR9 ligand CpG ODN 2216 as template. The homology search predicted a homologous CpG pattern in *P. vivax* showing 95% similarity with the template (Supplementary Table 1). This identified *P. vivax* CpG pattern was then used to derive the homologous CpG pattern from *L. mexicana* and *L. donovani*.

Recent reports on TLR9-CpG DNA interactions suggest that the helical B-conformation of ssDNA binds the TLR9 catalytic site [9,33]. Therefore we modeled the 3D structure of ODN and identified CpG DNA sequences as a single stranded molecule in the B-helical conformation for docking. The 3D structural complex of human and mouse TLR9 ECD with selected CpG DNA patterns demonstrated that the docked energy or ACE produced by the *L. donovani* CpG pattern and TLR9 complex was less than other complexes, indicating that this pattern has more robust protein ligand binding than other complexes. Moreover, the 14 parallel docking calculations with single base pair change at a time in the *L. donovani* CpG pattern predicted that the template fragment of *L. donovani* has the highest tendency toward TLR9 binding and this interaction is independent of single nucleotide differences. The hydrophobic and hydrogen bond interactions revealed that TLR9 ECD-CpG DNA interaction sites were located near the central region of the TLR9 ECDs. Hydrogen bonds are considered to be the chief mechanism behind the stable formation of a complex.

The predicted hydrogen bonds formed between TLR9 ECD–CpG DNA complexes (Supplementary Tables 4 and 5) revealed that the predicted *L. donovani* CpG DNA pattern had comparable predicted binding affinities to both hTLR9 and mTLR9 and that these were similar to the synthetic CpG ODN 2216 and other CpG DNA patterns studied. These findings support other studies that the identified *L. donovani* CpG DNA pattern for TLR9 activation is responsible for the Th1 immune response against the parasite. Furthermore, the molecular docking studies predicted that the LRR11 region of TLR9 remains conserved in terms of ligand recognition between mice and humans, indicating that recognition occurs across mammals. This notion supports the previous findings of Pan et al. that the positively charged residues of LRR11 are responsible for binding with the ligand [33]. To the best of our knowledge this is the first report regarding the theoretical identification and characterization of specific parasitic DNA patterns interacting with TLR9. The predicted CpG pattern of *L. donovani* can be employed as a synthetic immunomodulator, however experimental confirmation is required.

In conclusion, the proposed *Leishmania* CpG DNA sequences acting as ligands for TLR9 exhibited comparable theoretical interactions to known synthetic ODN. These findings can be applied to develop ideal innate immune generators against *Leishmania* parasitic infections. Our study supports that LRR11 of TLR9 ECD is responsible for ligand binding and provides a platform for designing novel immunomodulatory molecules as well as structural framework for interpreting existing and future experimental data.

Conflict of interest

None.

Acknowledgments

Department of Science & Technology, New Delhi, India is gratefully acknowledged for the financial support of this investigation as INSPIRE Fellowship to C.L.G (IF120575).

Appendix A. Supplementary data

Supplementary data related to this article can be found at http://dx.doi.org/10.1016/j.bbrc.2015.02.121.

Transparency document

Transparency document related to this article can be found online at http://dx.doi.org/10.1016/j.bbrc.2015.02.121.

References

[1] K. Takeda, S. Akira, Toll-like receptors in innate immunity, Int. Immunol. 17 (2005) 1–14.
[2] S. Uematsu, S. Akira, Toll-Like receptors (TLRs) and their ligands, Handb. Exp. Pharmacol. 183 (2008) 1–20.
[3] S. Akira, K. Takeda, Toll-like receptor signaling, Nat. Rev. Immunol. 4 (2004) 499–511.
[4] N.J. Gay, M. Gangloff, Structure and function of Toll receptors and their ligands, Annu. Rev. Biochem. 76 (2007) 141–165.
[5] C. Tsung-Hsien, J. Lee, L. Kline, et al., Toll-like receptor 9 mediates CpG-DNA signaling, J. Leukoc. Biol. 71 (2002) 538–544.
[6] G.M. Barton, R. Medzhitov, Toll-Like receptors and their ligands, Curr. Top. Microbiol. Immunol. 270 (2002) 81–92.
[7] M.S. Jin, J.O. Lee, Structures of TLR-ligand complexes, Curr. Opin. Immunol. 20 (2008) 414–419.
[8] T. Sparwasser, E.S. Koch, R.M. Vabulas, et al., Bacterial DNA and immunostimulatory CpG oligonucleotides trigger maturation and activation of murine dendritic cells, Eur. J. Immunol. 28 (1998) 2045–2054.
[9] W. Zhou, Y. Li, X. Pan, et al., Toll-like receptor 9 interaction with CpG ODN- an *in silico* analysis approach, Theor. Biol. Med. Model 10 (2013) 18.
[10] W.H.O., WHO Expert Committee Report on the Control of Leishmaniases, 2010, pp. 22–26. Geneva, March.
[11] T. Weinkopff, A. Mariotto, G. Simon, et al., Role of Toll-like receptor 9 signaling in experimental *Leishmania braziliensis* infection, Infect. Immun. 81 (2013) 1575.
[12] L. Monzote, Current treatment of leishmaniasis: a review, Open Antimicrob. Agents 1 (2009) 9–19.
[13] Y. Li, K. Ishii, H. Hisaeda, et al., IL-18 gene therapy develops Th1-type immune responses in Leishmania major-infected BALB/c mice: is the effect mediated by the CpG signaling TLR9? Gene Ther. 11 (2004) 941–948.
[14] F.F. Tuon, E.R. Fernandes, C. Pagliari, et al., The expression of TLR9 in human cutaneous leishmaniasis is associated with granuloma, Parasite Immunol. 32 (2010) 769–772.
[15] F.F. Tuon, V.S. Amato, H.A. Bacha, et al., Toll-like receptors and leishmaniasis, Infect. Immun. 76 (2008) 866–872.
[16] U. Schleicher, J. Liese, I. Knippertz, et al., NK cell activation in visceral leishmaniasis requires TLR9, myeloid DCs, and IL-12, but is independent of plasmacytoid DCs, J. Exp. Med. 204 (2007) 893–906.
[17] F.H. Abou Fakher, N. Rachinel, M. Klimczak, et al., TLR9-dependent activation of dendritic cells by DNA from Leishmania major favors Th1 cell development and the resolution of lesions, J. Immunol. 182 (2009) 1386–1396.
[18] B. Martinez-Salazar, M. Berzunza-Cruz, I. Becker, Leishmania mexicana DNA activates murine macrophages and increases their TLR9 expression, Gac. Med. Mex. 144 (2008) 99–104.
[19] M. Rutz, J. Metzger, T. Gellert, Toll-like receptor 9 binds single-stranded CpG-DNA in a sequence- and pH-dependent manner, Eur. J. Immunol. 34 (2004) 2541–2550.
[20] A. Roy, A. Kucukural, Y. Zhang, I-TASSER: a unified platform for automated protein structure and function prediction, Nat. Protoc. 5 (2010) 725–738.
[21] R.A. Laskowski, M.W. MacArthur, D.S. Moss, et al., PROCHECK: a program to check the stereochemical quality of protein structure, J. Appl. Crystallogr. 26 (1993) 283–291.
[22] G. Macindoe, L. Mavridis, V. Venkatraman, et al., HexServer: an FFT-based server powered by graphics processors, Nucleic Acids Res. 38 (2010) W445–W449.
[23] A.C. Wallace, R.A. Laskowski, J.M. Thornton, LIGPLOT: a program to generate schematic diagrams of protein-ligand interactions, Prot. Eng. 8 (1995) 127–134.
[24] D. Schneidman-Duhovny, Y. Inbar, R. Nussinov, et al., PatchDock and SymmDock: servers for rigid and symmetric docking, Nucleic Acids Res. 33 (2005) W363–W367.
[25] A. Levit, T. Yarnitzky, A. Wiener, et al., Modeling of human prokineticin receptors: interactions with novel small-molecule binders and potential off-target drugs, PLoS One 6 (2011) e27990.
[26] I. Buch, T. Giorgino, G. De Fabritiis, Complete reconstruction of an enzyme-inhibitor binding process by molecular dynamics simulations, Proc. Natl. Acad. Sci. U. S. A. 108 (2011) 10184–10189.
[27] M.E. Peter, A.V. Kubarenko, A.N.R. Weber, et al., Identification of an N-terminal recognition site in TLR9 that contributes to CpG-DNA-mediated receptor activation, J. Immunol. 182 (2009) 7690–7697.
[28] A.V. Kubarenko, S. Ranjan, A. Rautanen, et al., A naturally occurring variant in human TLR9, P99L, is associated with loss of CpG oligonucleotide responsiveness, J. Biol. Chem. 285 (2010) 36486–36494.
[29] M.S. Faria, F.C. Reis, A.P. Lima, Toll-like receptors in leishmania infections: guardians or promoters? J. Parasitol. Res. (2012), 930257.
[30] J. Liese, U. Schleicher, C. Bogdan, TLR9 signaling is essential for the innate NK cell response in murine cutaneous leishmaniasis, Eur. J. Immunol. 37 (2007) 3424–3434.
[31] A. Kuznik, M. Bencina, U. Svajger, et al., Mechanism of endosomal TLR inhibition by antimalarial drugs and imidazoquinolines, J. Immunol. 186 (2011) 4794–4804.
[32] J.D. Marshall, K. Fearon, C. Abbate, et al., Identification of a novel CpG DNA class and motif that optimally stimulate B cell and plasmacytoid dendritic cell functions, J. Leukoc. Biol. 73 (2003) 781–792.
[33] X. Pan, J. Yue, G. Ding, et al., Leucine-rich repeat 11 of Toll-like receptor 9 can Tightly bind to CpG-containing oligodeoxynucleotides, and the positively charged residues are critical for the high affinity, J. Biol. Chem. 287 (2012) 30596–30609.